Jahn-Teller distortion in Tris[4,4,4-Trifluoro-1-(2-thienyl)-1,3-butanedionato]manganese(III) isomers: an X-ray and computational study

Roxanne Gostynski,[a] Petrus H. van Rooyen,[b] Jeanet Conradie[a,*]

[a] Department of Chemistry, PO Box 339, University of the Free State, 9300 Bloemfontein, South Africa.

[b] Department of Chemistry, University of Pretoria, Private Bag X20, Hatfield, 0028, South Africa.

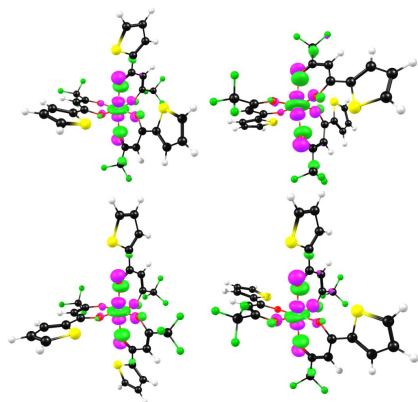*Contact author details:

Name: Jeanet Conradie

Tel: +27-51-4012194

e-mail: conradj@ufs.ac.za

Graphical abstract

Synopsis

Structure of $[Mn(CF_3COCHCOC_4H_3S)_3]$ isomers

Highlights

First crystal structure of a *mer* [Mn(β-diketonato)$_3$] complex

Crystal structure of Mn(III) with tetragonal elongated Jahn-Teller distortion

DFT geometries of one *fac* and three *mer* [Mn(CF$_3$COCHCOC$_4$H$_3$S)$_3$] isomers

Abstract

The solid state crystal data of a *mer* isomer of the [Mn(CF$_3$COCHCOC$_4$H$_3$S)$_3$] complex, [Mn(tfth)$_3$], exhibits elongation Jahn-Teller distortion (elongation of the metal-ligand bonds along the z-axis and shortening of the metal-ligand bonds along both the x and y-axes). Density functional theory calculations (DFT) show that one *fac* and three *mer* isomers of [Mn(tfth)$_3$] can exist. The difference between the three *mer* isomers of [Mn(tfth)$_3$] is that the Jahn-Teller elongation of the two *trans* axial Mn-O bonds along the z-axis occur along three different O$_{tfth}$-Mn-O$_{tfth}$ bonds. DFT calculations further show that the ground state geometry of all the [Mn(tfth)$_3$] isomers exhibits elongation Jahn-Teller distortion.

1   Introduction

Octahedral molecular geometry describes the shape of compounds wherein six atoms, or groups of atoms or ligands, are arranged symmetrically around a central atom. Octahedral complexes of high-spin manganese(III) are subjected to distortions, leading to deviations from the ideal octahedral molecular geometry [1]. Tris(β-diketonato)metal(III) complexes are octahedral complexes with an octahedral coordination polyhedron, MO$_6$. Possible distortions from the regular octahedral geometry for tris(β-diketonato)metal(III) complexes, include either elongation or compression along the tetragonal or z-axis, as well as orthorhombic distortion, leading to an asymmetric complex with two long, two medium and two small M-L bonds, see Scheme 1 (a). Crystal structures of different tris(β-diketonato)manganese(III) complexes exhibit elongation Jahn-Teller distortion [2,3,4] or compression Jahn-Teller distortion [5,6,7]. Reported structures of [Mn(acetylacetonato)$_3$] include three different crystalline forms: namely a β form obtained at room temperature, which exhibited a moderate compression (TC) of the metal-ligand bonds along the z-axis of about 0.05 Å [5]; secondly, a γ form, also obtained at room temperature (RT), which showed a significant elongation (TE) of the metal-ligand bonds along the z-axis of about 0.18 Å [2]; and thirdly, a δ form, obtained at low temperature (LT) (100K), exhibiting a Jahn-Teller orthorhombic distortion [8]. This result encouraged us to similarly determine the crystal structure of another [Mn(β-diketonato)$_3$] complex, at both RT and LT. This study therefore presents the crystal

structures of the [Mn(tfth)$_3$] complex, where tfth = (CF$_3$COCHCOC$_4$H$_3$S)$^-$, both at RT and at an LT of 150 K. The experimentally obtained crystal structures are complemented by a density functional theory study, to obtain insight into the electronic structure of this high spin 3d^4 Mn(III) complex. Since two isomers are possible for tris(β-diketonato)metal(III) complexes containing an unsymmetrical β-diketonato ligand (RCOCHCOR′)$^-$ (with different groups substituted on the ligand, R ≠ R′), namely a facial isomer (*fac*) and a meridional isomer (*mer*) (see Scheme 1 (b)), our aim was also to investigate which isomer would crystallize in the solid state.
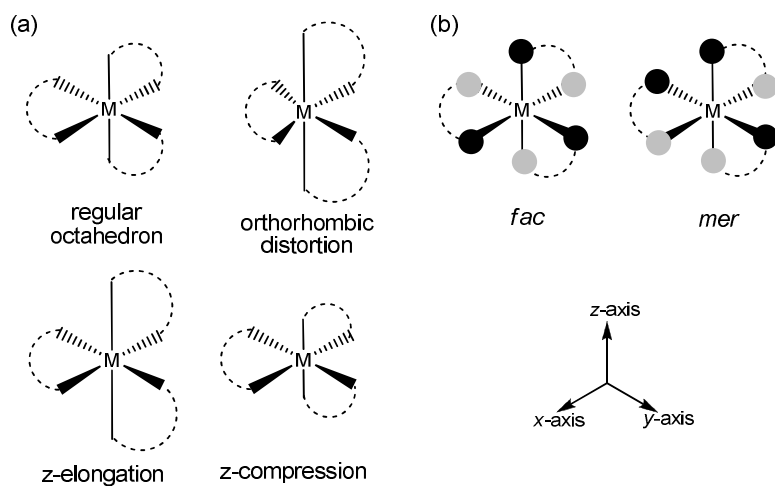
Scheme 1. (a) Possible distortions from the regular octahedral geometry, for tris(β-diketonato)metal(III) complexes. (b) Possible isomers for tris(β-diketonato)metal(III) complexes.

2 Experimental

2.1 Synthesis

Tris(thenoyltrifluoroacetone)manganese(III) was synthesized by a procedure adapted from literature [9], as reported previously [10]. The paramagnetic [Mn(tfth)$_3$] complex was characterized by MS, elemental analysis, UV/vis (supporting information Figure S2) and X-ray crystallography.

*Characterization data for [Mn(CF$_3$COCHCOC$_4$H$_3$S)$_3$], (**6**) [Mn(tfth)$_3$]*

Yield 97 %. Colour: Brown. Melting point 157.5 °C. MS Calculated: Mr = 718.45 g/mol, Found: 718.72 g/mol. Elemental analysis, calculated for MnC$_{24}$H$_{12}$O$_6$F$_6$S$_3$: C, 40.1; H, 1.7, Found: C, 40.7; H, 1.99.

2.2 Crystal structure analysis

Data for the crystals, obtained from solutions in diethyl ether, were collected on a Bruker D8 Venture kappa geometry diffractometer, with duo Iµs sources, a Photon 100 CMOS detector and APEX II [11] control software, using Quazar multi-layer optics, monochromated Mo-$K\alpha$ radiation, by means of a combination of ϕ and ω scans. Data reduction was performed using SAINT+ [11] and the intensities were corrected for absorption using SADABS [11]. The structure was solved by intrinsic phasing using SHELXTS and refined by full-matrix least squares, using SHELXTL + [12] and SHELXL-2015+ [12]. In the structure refinement, all the aromatic hydrogen atoms were added in calculated positions and treated as riding on the atom to which they are attached. All non-hydrogen atoms were refined with anisotropic displacement parameters; all isotropic displacement parameters for hydrogen atoms were calculated as $X \times U_{eq}$ of the atom to which they are attached, where $X = 1.2$. Crystal data and structural refinement parameters are given in the electronic supplementary information. Crystallographic data has been deposited at the Cambridge Crystallographic Data Centre, with numbers: 1449937-1449938.

2.3 Density functional theory (DFT) calculations

Density functional theory (DFT) calculations were carried out, using the ADF (Amsterdam Density Functional) 2013 programme [13], with a selection of GGA (Generalized Gradient Approximation) functionals, namely PW91 (Perdew-Wang 1991) [14], BP86 (Becke-Perdew) [15,16], and OLYP (Handy-Cohen and Lee-Yang-Parr) [17,18], S12g [19], OPBE [20], the meta-GGA functional M06-L [21], as well as the hybrid functionals B3LYP (Becke 1993 and Lee-Yang-Parr) [22,23], O3LYP [24], B3LYP* [25] and S12h [19]. The TZP (Triple ζ polarized) basis set, with a fine mesh for numerical integration and full geometry optimization, applying tight convergence criteria, was used for minimum energy searches.

3 Results and Discussion

3.1 X-ray structure

The crystal data and structure refinement details of the [Mn(tfth)$_3$] crystal in this study, performed at both RT and at a LT of 150 K, are given in the Supporting Information. Figure 1 and Figure 2 present perspective drawings [26] of the molecular structure of the *mer* isomer of [Mn(tfth)$_3$], obtained at 296 K (RT) and at 150 K (LT), showing the crystallographic numbering

scheme used. Table 1 gives selected geometrical parameters of [Mn(tfth)$_3$] and other published [Mn(III)(β-diketonato)$_3$] complexes. Both the RT and LT [Mn(tfth)$_3$] structure crystallize in the P2$_1$/n space group, with Z = 4. Two *trans* Mn-O bond lengths are longer than the other four Mn-O bond lengths; therefore, both the RT and LT crystal structures can be described as elongation Jahn-Teller distortion. The distortion of the coordination polyhedron from a regular octahedron is due to the Jahn-Teller effect for the high-spin 3d^4 Mn(III) ion in [Mn(tfth)$_3$], with a degenerate occupancy of the e$_g$ subshell in an octahedral environment. The average lengths of the four "short" equatorial and the two "long" tetragonal Mn-O bonds in the two structures are 1.921(4) and 2.103(4) Å at RT, and 1.914(4) and 2.135(4) Å at LT, respectively. The difference between these average Mn-O bond lengths is 0.182 for the RT structure, and 0.221 Å for the LT structure, respectively (see Table 1), which clearly indicates elongation Jahn-Teller distortions. Upon lowering temperature from RT to 150 K, the two longer Mn-O bonds increased in length by *ca.* 0.03 Å (from 2.096(4) and 2.109(4) Å at RT, to 2.128(4) and 2.141(4) at 150 K). It can therefore be seen that [Mn(tfth)$_3$] exhibits appreciable elongation Jahn-Teller distortion at low temperature.

The packing diagram of [Mn(tfth)$_3$] (at 150 K) is presented in Figure S1 in the Supporting Information. Due to the significant rotational motion of the CF$_3$ groups in the RT structure, the fluorine atoms have large anisotropic displacement parameters relative to those found in the LT structure. The three crystallographically independent cyclic β-diketonato ligands which include Mn, in the *mer* isomer of [Mn(tfth)$_3$], are ring1 (Mn1-O1-C1-C2-C3-O2), ring2 (Mn1-O3-C4-C5-C6-O4) and ring3 (Mn1-O5-C7-C8-C9-O6). These rings are planar, with the largest deviations from planarity being 0.036(4) Å (RT) and 0.032(4) Å (LT) for the O1 atom in ring1, 0.188(4) Å (RT) and 0.194(3) Å (LT) for the O4 atom in ring2, and 0.112(1) Å (RT) and 0.116(1) Å (LT) Å for the metal Mn1 in ring3. The angles between the mean planes through these three rings, in both the RT and the LT structures, vary between 78.46(17)° and 84.45(18)°. In each case, these three rings are planar with the thiophene rings attached to them, with the largest deviation from planarity being 5.3(3)°. The thiophene rings are labelled ring4, ring5 and ring6, and are attached to the β-diketonato ligands ring1, ring2 and ring3, respectively. Some parallel π-stacking effects are observed, with the shortest intermolecular π-π (parallel) distances being those of ring4---ring5 [3.843(4) Å (RT) and 3.815(4) Å (LT)]; ring5---ring5 [3.639(4) Å (RT) and 3.640(4) Å (LT)]; and ring6---ring6 [3.843(4) Å (RT) and 3.815(4) Å (LT)]. In addition, a stabilizing H-interaction with a π-system is also observed for the perpendicular C21-H21...ring4 interaction, of 2.820 Å (RT) and 2.840 Å (LT). However, the only significant intermolecular F---H interaction observed is that between F9 and H14 (2.60 Å in the LT structure).

All currently published crystal structures of [Mn(β-diketonato)$_3$] complexes contain a symmetrical β-diketonato ligand (RCOCHCOR')$^-$, with substituents R = R', see Table 1. The

structure of the *mer*-[Mn(tfth)$_3$] isomer with elongation Jahn-Teller distortion presented in this study, is the first [Mn(β-diketonato)$_3$] structure containing an unsymmetrical β-diketonato ligand (RCOCHCOR')⁻, with substituents R ≠ R'. The published structures of [Mn(acac)$_3$] (Hacac = acetylacetone = CH$_3$COCH$_2$COCH$_3$) include structures with elongation Jahn-Teller distortion, compression Jahn-Teller distortion and orthorhombic distortion. However, high-frequency and high-field electron paramagnetic resonance (HFEPR) spectroscopy of [Mn(acac)$_3$], obtained in frozen solution, free of crystal packing effects, indicated that axial elongation could be considered the "natural" form of Jahn-Teller distortion for octahedral high-spin 3d^4 ions. The moderately compressed Jahn-Teller distortion also found for [Mn(acac)$_3$], is considered an unusual consequence of unknown crystal packing effects [27]. The three published structures of [Mn(dbm)$_3$] (Hdbm = dibenzoylmethane = PhCOCH$_2$COPh) obtained at RT and 100K, clearly showed elongation Jahn-Teller distortion, with the difference between the average lengths for the four "short" and two "long" trans Mn-O bonds larger than 0.20 Å. Crystallographic data of [Mn(dpm)$_3$] (Hdpm = dipivaloymethane = ^{t}BuCOCH$_2$CO^{t}Bu) at 153 K, show compression Jahn-Teller distortion, with the difference between the average lengths for the four "long" and two "short" trans Mn-O bonds equal to 0.13 Å.
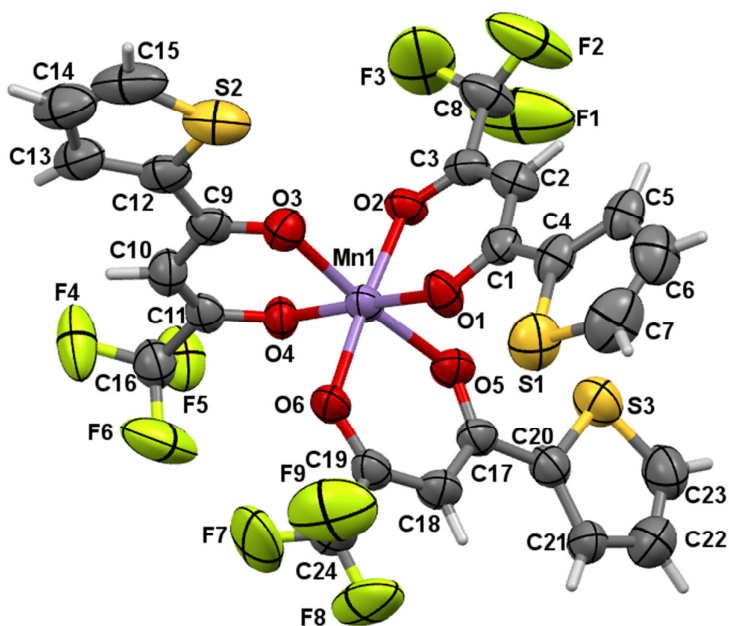

Figure 1: A perspective drawing of the molecular structure of *mer*-[Mn(tfth)$_3$], obtained at RT of 296 K, showing the atom numbering scheme. Atomic displacement parameters (ADPs) are shown at the 50 % probability level.
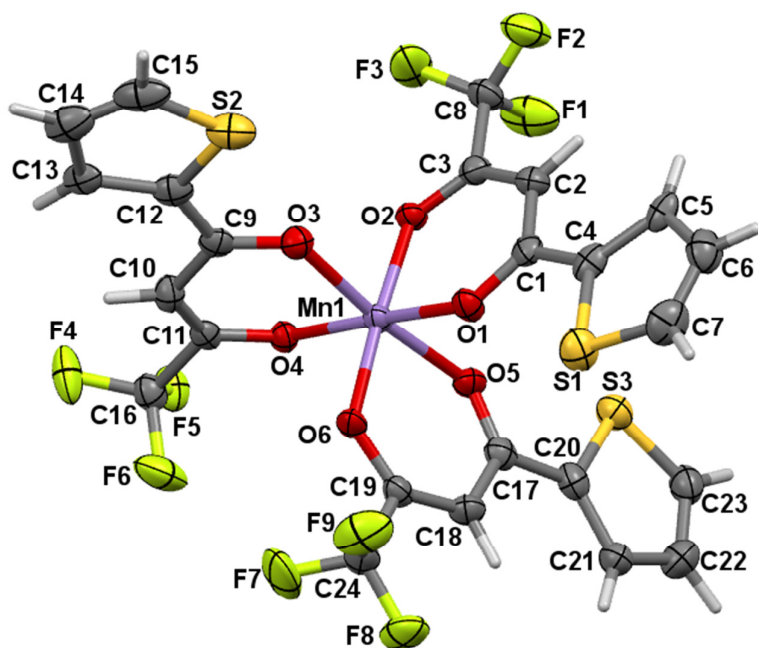
Figure 2: A perspective drawing of the molecular structure of *mer*-[Mn(tfth)$_3$], obtained at an LT of 150 K, showing the atom numbering scheme. Atomic displacement parameters (ADPs) are shown at the 50 % probability level.

Table 1: Selected geometric parameters for [Mn(III)(β-diketonato)$_3$] complexes.

β-diketonato	Mn–O (Å) 1	2	3	4	5	6	Distortion	Distortion amount (Å)[a]	CSD ref code	Ref	Temp
acac	1.931(10)	1.956(7)	1.984(8)	1.991(7)	2.003(8)	2.020(7)	moderate compression	0.05	ACACMN02	5	RT
	1.936(5)	1.950(5)	1.983(5)	1.987(5)	2.014(5)	2.018(5)	elongation	0.18	ACACMN21	2	RT
	1.931(3)	1.933(3)	1.934(4)	1.942(3)	2.109(3)	2.112(4)	elongation	0.16	ACACMN21	2	RT
	1.895(8)	1.937(8)	2.004(11)	2.006(10)	2.034(9)	2.046(8)	not clear[b]	-	ACACMN23	8	293 K
	1.926(8)	1.951(8)	2.010(11)	2.023(9)	2.024(9)	2.034(11)	not clear[b]	-	ACACMN23	8	293 K
	1.964(8)	1.966(10)	1.976(9)	1.984(8)	2.020(11)	2.046(12)	not clear[b]	-	ACACMN23	8	293 K
	1.959(9)	1.984(10)	1.989(9)	1.999(11)	2.012(8)	2.028(11)	not clear[b]	-	ACACMN23	8	293 K
	1.901(2)	1.930(2)	1.976(2)	1.984(2)	2.106(2)	2.111(2)	orthorhombic	-	ACACMN22	8	100 K
	1.914(2)	1.926(2)	1.981(2)	1.984(2)	2.082(2)	2.090(2)	orthorhombic	-	ACACMN22	8	100 K
	1.940(3)	1.945(3)	1.957(3)	1.958(3)	2.060(3)	2.078(4)	slight elongation	0.12	XESPIW	28	RT
dbm	1.904(1)	1.915(1)	1.920(1)	1.924(1)	2.122(1)	2.160(1)	elongation	0.23	JINPIF02	29	100 K
	1.89(2)	1.91(2)	1.92(2)	1.93(2)	2.09(2)	2.13(3)	elongation	0.20	JINPIF	3	RT
	1.908(2)	1.917(2)	1.931(2)	1.935(2)	2.109(2)	2.142(2)	elongation	0.20	JINPIF01	4	RT
	1.902(3)	1.927(3)	1.930(3)	1.941(4)	2.116(3)	2.141(4)	elongation	0.20	NOSHUA	30	RT
dpm	1.901	1.901	2.028	2.028	2.036	2.036	compression	0.13	QAYYEU	7	153 K
tfth	1.908(3)	1.921(4)	1.923(4)	1.931(4)	2.096(4)	2.109(4)	elongation	0.18	-	this study	RT
tfth	1.904(4)	1.912(3)	1.919(4)	1.920(3)	2.128(4)	2.141(4)	elongation	0.22	-	this study	150 K

a The difference between the four longest and two shortest bonds for elongation, and between the four shortest and two longest bonds for compression Jahn-Teller distortion.

b The standard deviation on inter atomic distances is too large.

3.2 Computational chemistry study

To validate the computational chemistry approach, the different electronic states of [Mn(acac)$_3$] (the best-known [Mn(β-diketonato)$_3$] complex), were optimized. **Table 2** gives the DFT calculated energies of the spin states $S = 1$ and $S = 2$ of [Mn(acac)$_3$], optimized via a selection of different types of DFT functionals, namely the GGA functionals PW91, BP86, OLYP, OPBE, S12g, the meta-GGA functional M06-L and the hybrid functionals O3LYP, B3LYP, B3LYP*, S12h. The $S = 0$ closed shell state could not be optimized. These results indicate that the OLYP, OPBE, M06-L, S12h, B3LYP, B3LYP* functionals correctly predicted the experimental high state of $S = 2$ (four unpaired electrons) [4,31] of [Mn(acac)$_3$]. The electronic ground state of high-spin [Mn(acac)$_3$] is $d_{xy}^1 d_{xz}^1 d_{yz}^1 d_{z2}^1$ [32], implying that only one of the two d orbitals in the e_g set (d_{x2-y2} and d_{z2}) of an octahedral environment is occupied. The Jahn-Teller theorem states that in molecules that have a degenerate ground-state, the molecule will distort to remove the degeneracy. This implies that, since the e_g orbital set for [Mn(acac)$_3$] is partially occupied, the molecule will be distorted, in order to lower the energy of the molecule [1]. Thus, all [Mn(β-diketonato)$_3$] complexes exhibit Jahn-Teller distortion. The DFT calculated minimum energy electronic ground state ($d_{xy}^1 d_{xz}^1 d_{yz}^1 d_{z2}^1$) of [Mn(acac)$_3$], exhibits elongation Jahn-Teller distortion, with two tetragonal axial Mn-O bonds along the z-axis, which are longer than the other four equatorial bonds in the xy-plane [32].

Table 3 gives the energies of the *fac* and *mer*-[Mn(tfth)$_3$] isomers, obtained via a selection of functionals that correctly predicted the $S = 2$ ground state of [Mn(acac)$_3$], namely OLYP, OPBE, B3LYP and B3LYP*. All the isomers have an electronic ground state of $d_{xy}^1 d_{xz}^1 d_{yz}^1 d_{z2}^1$, with elongation Jahn-Teller distortion. The Jahn-Teller elongation of the two trans axial Mn-O bonds along the z-axis for the *mer*-[Mn(tfth)$_3$] isomers, can occur along any of the three different O$_{tfth}$-Mn-O$_{tfth}$ bonds, leading to three different elongation *mer*-[Mn(tfth)$_3$] isomers, namely the *mer*-Th-Th, *mer*-Th-CF$_3$ and *mer*-CF$_3$-CF$_3$ isomers, named to indicate the groups attached to the two trans β-diketonato ligands along the z-axis, see **Figure 3** for OLYP/TZP optimized geometries (CF$_3$ and Th = C$_4$H$_3$S). The crystal structures presented in the previous section were the *mer*-Th-Th isomers, in agreement with the OLYP/TZP lowest energy structure. However, the small energy difference between the different isomers (**Table 3**) indicates that all these isomers can exist. The four isomers are therefore proposed to be in equilibrium with each other.

To further validate the computational chemistry approach, the average experimental Mn–O bond lengths for the four "short" equatorial and the two "long" tetragonal Mn-O bonds in the RT and LT experimental structures, are compared with the DFT calculated values in **Table 4**. Better

agreement is obtained between the calculated structures and the LT experimental structure than with the RT experimental structure. However, the LT experimental structure is still slightly overestimated by 0.02 – 0.04 Å by the calculated bond lengths. Gas phase calculations as well as GGA density functionals generally tend to overestimate bond lengths [33]; for example, longer calculated bond lengths, compared to crystallographic measured bond lengths, have also been found for related [M(β-diketonato)$_3$] complexes with M = Mn [29], Fe [34], Co [35], Cr [35] and rhodium-β-diketonato complexes [36,37]. Since the difference between the average experimental Mn–O bond lengths for the four "short" equatorial and the two "long" tetragonal Mn-O bonds in the RT and LT experimental structures differ by 0.01 – 0.03 Å, all the DFT methods used here are considered to give good agreement with experimental geometries.

The HOMOs (highest occupied molecular orbitals) of the [Mn(tfth)$_3$] isomers in **Figure 3**, give insight into the observed elongation along the z-axis. The HOMOs are mainly of d_{z2} character and the lobes of the d_{z2} orbital point directly to the p_z orbital on the O_{tfth} atom. Repulsion between these orbitals leads to elongation of the Mn-O_{tfth} bonds along the z-axis.

Table 2: Relative energies (eV) of the different spin states of [Mn(acac)$_3$], optimized via a selection of functionals. The lowest energy is indicated in bold as 0.

Spin[a]	PW91	BP86	O3LYP	S12g	S12h	OLYP	OPBE	B3LYP	B3LYP*	M06-L
1	**0.000**	**0.000**	**0.000**	**0.000**	0.682	0.327	0.322	0.274	0.140	0.394
2	0.307	0.267	0.388	0.000	**0.000**	**0.000**	**0.000**	**0.000**	**0.000**	**0.000**

a Spin $S = 0$ could not be optimized.

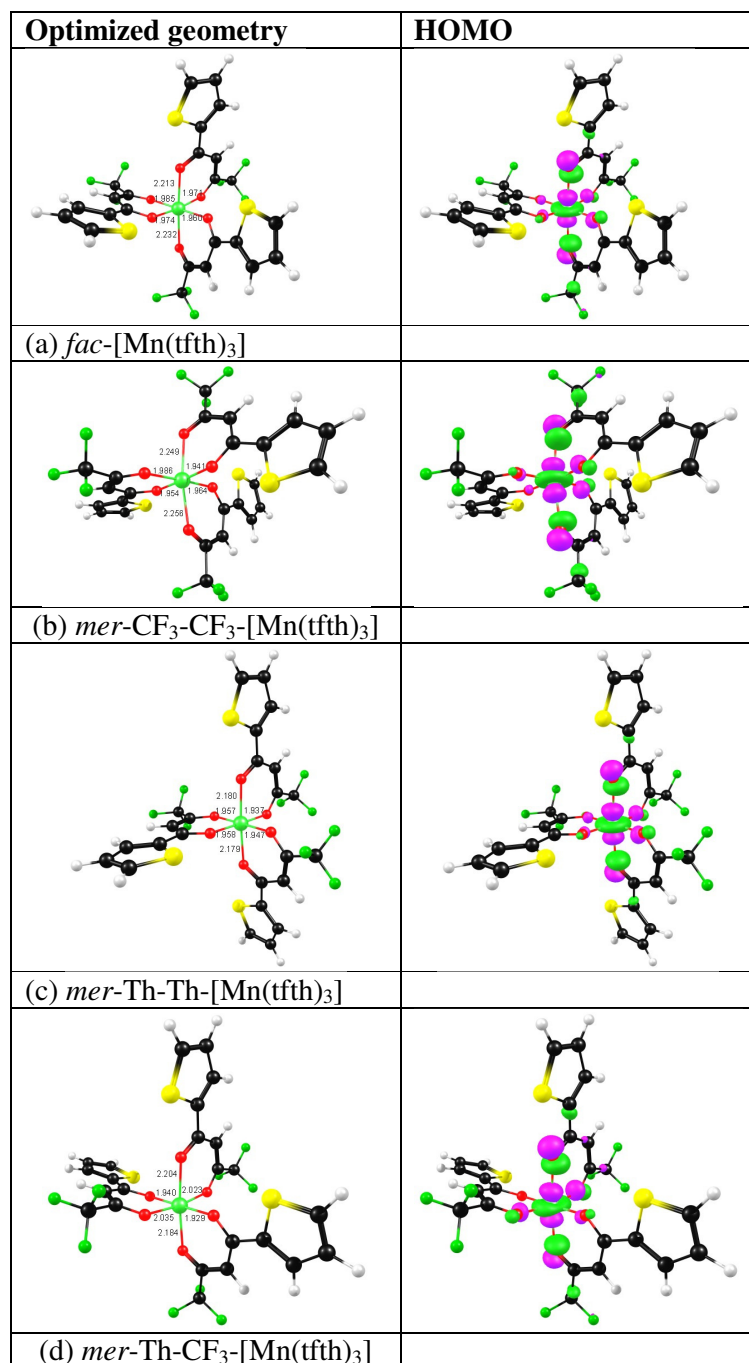| Optimized geometry	HOMO
(a) *fac*-[Mn(tfth)₃]	
(b) *mer*-CF₃-CF₃-[Mn(tfth)₃]	
(c) *mer*-Th-Th-[Mn(tfth)₃]	
(d) *mer*-Th-CF₃-[Mn(tfth)₃]	

Figure 3: The OLYP/TZP optimized geometry (left) and HOMO (right) of the one *fac* and three *mer*-[Mn(tfth)₃] isomers of complex [Mn(tfth)₃].

Table 3: Relative energies (eV) of the lowest energy $d_{xy}^1 d_{xz}^1 d_{yz}^1 d_{z2}^1$ ground state of [Mn(tfth)$_3$] isomers, obtained via a selection of functionals. The lowest energy is indicated in bold as 0.

Isomer	OLYP	OPBE	B3LYP	B3LYP*
fac	0.090	0.070	0.108	0.110
mer CF$_3$-CF$_3$	0.016	**0.000**	0.012	0.011
mer CF$_3$-Th	0.025	0.011	**0.000**	**0.000**
mer Th-Th (experimental structure)	**0.000**	0.030	0.007	0.013

Table 4: Average experimental and DFT calculated Mn–O bond lengths (Å) for the four "short" equatorial and the two "long" tetragonal Mn-O bonds in *mer*-Th-Th-[Mn(tfth)$_3$].

	Average Mn-O bonds (Å)		Difference: calc. and RT exp. structure		Difference: calc. and LT exp. structure	
	4 short	2 long	4 short	2 long	4 short	2 long
OLYP calc.	1.950	2.179	0.03	0.08	0.04	0.04
OPBE calc.	1.949	2.179	0.03	0.08	0.04	0.04
B3LYP calc.	1.947	2.155	0.03	0.05	0.03	0.02
B3LYP* calc.	1.948	2.153	0.03	0.05	0.03	0.02
PW91 calc.	1.946	2.175	0.03	0.07	0.03	0.04
exp RT	1.921(4)	2.103(4)	-	-	0.01[a]	-0.03[a]
exp LT	1.914(4)	2.135(4)	-0.01[a]	0.03[a]	-	-

a Difference: LT and RT exp. structure

4 Conclusion

Density functional theory calculations (DFT) show that the *fac* and *mer* isomers of tris(thenoyltrifluoroacetone-κ^2O,O')manganese(III) have an electronic configuration of $d_{xy}^1 d_{xz}^1 d_{yz}^1 d_{z2}^1$, with elongation Jahn-Teller distortion. DFT calculations further show that one *fac* and three *mer* isomers of [Mn(tfth)$_3$] can exist, with the four isomers in equilibrium with one another. The solid state crystal structure of *mer*-[Mn(CF$_3$COCHCOC$_4$H$_3$S)$_3$], [Mn(tfth)$_3$], exhibits elongation Jahn-Teller distortion, both at room temperature and at 150 K.

Supporting Information

Crystallographic data has been deposited at the Cambridge Crystallographic Data Centre, with numbers: 1449937-1449938. Copies can be obtained, free of charge, on application to CCDC, 12 Union Road, Cambridge CB2 1EZ, UK [fax: +44 (0)1223 336033 or www.ccdc.cam.ac.uk/products/csd/request/]. Selected crystallographic data and the optimized coordinates of the DFT calculations are given in the Supporting Information.

References

[1] H.A. Jahn, E. Teller, Stability of Polyatomic Molecules in Degenerate Electronic States. I. Orbital Degeneracy, Proc. R. Soc. Lond. A 161 (1937) 220–235. DOI: 10.1098/rspa.1937.0142

[2] B.R. Stults, R.S. Marianelli, V.W. Day, Distortions of the coordination polyhedron in high-spin manganese(III) complexes. 3. Crystal and molecular structure of gamma-tris(acetylacetonato)manganese(III): a tetragonally elongated octahedral form, Inorg. Chem. 18 (1979) 1853–1858.

[3] E.G. Zaitseva, I.A. Baidina, P.A. Stabnikov, S.V. Borisov, I.K. Igumenov, Crystal and molecular structure of tris(dibenzoylmathanato)manganese(III), Zh. Strukt. Khim. (Russ.) (Russian Journal of Structural Chemistry) 31 (1990) 349-357. (CCDC reference JINPIF)

[4] A.L. Barra, D. Gatteschi, R. Sessoli, G.L. Abbati, A. Cornia, A.C. Fabretti, M.G. Uytterhoeven, Electronic Structure of Manganese(III) Compounds from High-Frequency EPR Spectra, Angew. Chem. Int. Ed. 36 (1997) 2329-2331. (CCDC 406981, reference JINPIF01)

[5] J.P. Fackler, A. Avdeef, Crystal and molecular structure of tris(2,4-pentanedionato) manganese(III), $Mn(O_2C_5H_7)_3$, a distorted complex as predicted by Jahn-Teller arguments, Inorg. Chem. 13 (1974) 1864–1875.

[6] R. Frohlich, R. Milan, S. Yadava, CCDC 692561, reference ACACMN24, Private communication (2008).

[7] P. Magnus, A.H. Payne, M.J. Waring, D.A. Scott, V. Lynch, Conversion of α,β-unsaturated ketones into α-hydroxy ketones using an Mn[III] catalyst, phenylsilane and dioxygen: acceleration of conjugate hydride reduction by dioxygen, Tetrahedron Lett. 41 (2000) 9725-9730. (CCDC 158103, reference QAYYEU)

[8] S. Geremia, N. Demitri, Crystallographic Study of Manganese(III) Acetylacetonate: An Advanced Undergraduate Project with Unexpected Challenges, J. Chem. Educ. 82 (2005) 460-465.

[9] M.N. Bhattacharjee, M.K. Chaudhuri, D.T. Khathing, Direct Synthesis of Tris(acetylacetonato)manganese(III), Dalton Trans. (1982) 669-670.

[10] R. Freitag, J. Conradie, Electrochemical and Computational Chemistry Study of Mn(β-diketonato)$_3$ complexes, Electrochim. Acta, 158 (2015) 418-426.

[11] APEX2 (including SAINT and SADABS), Bruker AXS Inc., Madison, WI, 2012.

[12] G.M. Sheldrick, A short history of SHELX, Acta Cryst. A64 (2008) 112-122.

[13] G. te Velde, F.M. Bickelhaupt, E.J. Baerends, C.F. Guerra, S.J.A. van Gisbergen, J.G. Snijders, T. Ziegler, Chemistry with ADF, J. Comput. Chem. 22 (2001) 931-967.

[14] J.P. Perdew, J.A. Chevary, S.H. Vosko, K.A. Jackson, M.R. Pederson, D.J. Singh, C. Fiolhais, Atoms, molecules, solids, and surfaces: Applications of the generalized gradient approximation for exchange and correlation, Phys. Rev. B46 (1992) 6671-6687. Erratum: J.P. Perdew, J.A. Chevary, S.H. Vosko, K.A. Jackson, M.R. Perderson, D.J. Singh, C. Fiolhais, Phys. Rev. B48 (1993) 4978.

[15] A.D. Becke, Density-functional exchange-energy approximation with correct asymptotic behavior, Phys. Rev. A38 (1988) 3098-3100.

[16] J.P. Perdew, Density-functional approximation for the correlation energy of the inhomogeneous electron gas, Phys. Rev. B33 (1986) 8822-8824; J.P. Perdew, Erratum: Density-functional approximation for the correlation energy of the inhomogeneous electron gas: Phys. Rev. B34 (1986) 7406.

[17] N.C. Handy, A.J. Cohen, Left-right correlation energy, Mol. Phys. 99 (2001) 403-412.

[18] (a) C. Lee, W. Yang, R.G. Parr, Development of the Colle-Salvetti correlation-energy formula into a functional of the electron density, Phys. Rev. B 37 (1988) 785-789. (b) B.G. Johnson, P.M.W. Gill, J.A. Pople, The performance of a family of density functional methods, J. Chem. Phys. 98 (1993) 5612-5626. (c) T.V. Russo, R.L. Martin, P.J. Hay, Density functional calculations on first-row transition metals, J. Chem. Phys. 101 (1994) 7729-7737.

[19] M. Swart, A new family of hybrid density functionals, Chem. Phys. Lett. 580 (2013) 166-171.

[20] M. Swart, A.W. Ehlers, K. Lammertsma, Performance of the OPBE exchange-correlation functional, Mol. Phys. 102 (2004) 2467-2474.

[21] (a) Y. Zhao, D.G. Truhlar, A new local density functional for main-group thermochemistry, transition metal bonding, thermochemical kinetics, and noncovalent interactions, J. Chem. Phys. 125 (2006) 194101-194118. (b) Y. Zhao, D.G. Truhlar, The M06 suite of density functionals for main group thermochemistry, thermochemical kinetics, noncovalent interactions, excited states, and transition elements: two new functionals and systematic testing of four M06-class functionals and 12 other functionals, Theor. Chem. Account 120 (2008) 215-241.

[22] A.D. Becke, Density-functional thermochemistry. III. The role of exact exchange, J. Chem. Phys. 98 (1993) 5648-5652.

[23] P.J. Stephens, F.J. Devlin, C.F. Chabalowski, M.J. Frisch, Ab Initio Calculation of Vibrational Absorption and Circular Dichroism Spectra Using Density Functional Force Fields, J. Phys. Chem. 98 (1994) 11623-11627.

[24] A.J. Cohen, N.C. Handy, Dynamic correlation, Mol. Phys. 99 (2001) 607-615.

[25] M. Reiher, O. Salomon, B.A. Hess, Reparameterization of hybrid functionals based on energy differences of states of different multiplicity, Theor. Chem. Account 107 (2001) 48-55.

[26] L.J. Farrugia, WinGX and ORTEP for Windows: an update, J. Appl. Crystallogr. 45 (2012) 849-854.

[27] J. Krzystek, G. Yeagle, J-H. Park, R.D. Britt, M.W. Meisel, L-C. Brunel, J. Telser, High-Frequency and -Field EPR Spectroscopy of Tris(2,4-pentanedionato)manganese(III): Investigation of Solid-State versus Solution Jahn-Teller Effects, Inorg. Chem. 42 (2003) 4610-4618.

[28] Y. Cheng, S. Xia, J. Feng, S. Du, L. An, X. Lu, Solvothermal Synthesis and Crystal Structures of Two Manganese Complexes $[Mn(II)(acac^-)_2(4,4'-bipy)]_n$ (bipy = 4,4'-bipyridine) and $[Mn(III)(acac^-)_3]•4CO(NH_2)_2$, Chin. J. Chem. 30 (2012) 1063-1068.

[29] R. Freitag, T.J. Muller, J. Conradie, X-ray diffraction and DFT calculation elucidation of the Jahn-Teller effect observed in $Mn(dibenzoylmethanato)_3$, J. Chem. Cryst. 44 (2014) 352-359.

[30] L. Chen, J. Wang, Y-Z. Liu, Y. Song, X-T. Chen, Y-Q. Zhang, Z-L. Xue, Slow Magnetic Relaxation in Mononuclear Octahedral Manganese(III) Complexes with Dibenzoylmethanide Ligands, Eur. J. Inorg. Chem. 2 (2015) 271-278.

[31] S.L. Dexheimer, J.W. Gohdes, M.K. Chan, K.S. Hagen, W.H. Armstrong, M.P. Klein, Detection of EPR Spectra in S = 2 States of Trivalent Manganese Complexes, J. Am. Chem. Soc. 111 (1989) 8923-8926.

[32] R. Freitag, J. Conradie, Understanding the Jahn-Teller Effect in octahedral transition metal complexes – a Molecular Orbital view of the Mn(β-diketonato)$_3$ complex, J. Chem. Educ. 90 (2013) 1692-1696.

[33] (a) A.C. Scheiner, J. Baker, J.W. Andzelm, J. Comput. Chem. 18 (1997) 775. (b) J.R. Hill, C.M. Freeman, B. Delley, J. Phys. Chem. A, 103 (1999) 3772. (c) F. Furche, J.P. Perdew, J. Chem Phys. 124 (2006) 044103.

[34] M.M. Conradie, P.H. van Rooyen, J. Conradie, Crystal and electronic structures of Tris[4,4,4-Trifluoro-1-(2-X)-1,3-butanedionato]iron(III) isomers (X = thienyl or furyl): an X-ray and computational study, J. Mol. Struct. 1053 (2013) 134-140.

[35] R. Liu, P.H. van Rooyen, J. Conradie, Geometrical isomers of Tris(beta-diketonato)metal(III) complexes for M = Cr or Co: synthesis, X-ray structures and DFT study, Inorg. Chim. Acta 477 (2016) 59-65.

[36] M.M. Conradie, J. Conradie, Stereochemistry of the Reaction Products of the Oxidative Addition Reaction of Methyl Iodide to [Rh((C$_4$H$_3$S)COCHCOR)(CO)(PPh$_3$)]: a NMR and Computational Study. R = CF$_3$, C$_6$H$_5$, C$_4$H$_3$S, Inorg. Chim. Acta 362 (2009) 519-530.

[37] M.M. Conradie, J. Conradie, Methyl Iodide Oxidative Addition to Rhodium(I) Complexes: a DFT and NMR Study of [Rh(FcCOCHCOCF$_3$)(CO)(PPh$_3$)] and the Rhodium(III) Reaction Products, S. Afr. J. Chem.61 (2008) 102-111.